Available online at www.sciencedirect.com
ScienceDirect
Journal of Hazardous Materials 146 (2007) 529–534
Journal of Hazardous Materials
www.elsevier.com/locate/jhazmat

Photocatalytic activity of TiO_2 doped with boron and vanadium

M. Bettinelli [a,*], V. Dallacasa [b,**], D. Falcomer [a], P. Fornasiero [c,***], V. Gombac [c], T. Montini [c], L. Romanò [d], A. Speghini [a]

[a] Dipartimento Scientifico e Tecnologico, Università di Verona, and INSTM, UdR Verona, Ca' Vignal, Strada Le Grazie 15, 37134 Verona, Italy
[b] Laboratory of Materials Analysis, Dipartimento Scientifico e Tecnologico, Università di Verona, Ca' Vignal, Strada Le Grazie 15, 37134 Verona, Italy
[c] Dipartimento di Scienze Chimiche, Università di Trieste, CENMAT and INSTM, UdR Trieste, Via Giorgieri 1, 34127 Trieste, Italy
[d] Dipartimento di Fisica, Università di Parma, Viale G. P. Usberti 7/A, 43100 Parma, Italy

Available online 20 April 2007

Abstract

Boron (B)- and vanadium (V)-doped TiO_2 photocatalysts were synthesized using modified sol–gel reaction processes and characterized by X-ray diffraction (XRD), Raman spectroscopy and N_2 physisorption (BET). The photocatalytic activities were evaluated by monitoring the degradation of methylene blue (MB). The results showed that the materials possess high surface area. The addition of B favored the transformation of anatase to rutile, while in the presence of V, anatase was the only phase detected. The MB degradation on V-doped TiO_2 was significantly affected by the preparation method. In fact while the presence of V in the bulk did not influence strongly the photoreactivity under visible irradiation, an increase of surface V doping lead to improved photodegradation of MB. The degradation of MB dye indicated that the photocatalytic activities of TiO_2 increased as the boron doping increased, with high conversion efficiency for 9 mol% B doping.

Keywords: TiO_2; Doping; Methylene blue photodegradation; Boron; Vanadium

1. Introduction

Titanium dioxide (TiO_2) has attracted growing scientific interest for its good performances in photocatalytic oxidation of organic molecules, for its application in solar cells, thin-film optical devices, and as gas sensor [1]. TiO_2 mediated photooxidation is indeed used for environmental remediation [2], where toxic materials at low concentration are converted, in a series of chemical steps, to harmless oxidation products such CO_2 and H_2O. Honda and Fujishima have evidenced the photocatalytic activity of TiO_2 since the pioneering studies of water reduction through photoexcitation of TiO_2 in 1972 [3].

Interestingly, according to many reports [1,4,5] the activity of anatase phase of TiO_2 in the photodegradation of various pollutants is, in general, much higher than that of rutile. It has been shown that the photocatalytic activity of TiO_2 is influenced by crystal structure, surface area, crystallinity and porosity [5]. Many approaches have been used to obtain nanosized samples phase of anatase titania, such as chemical vapor synthesis [5], the sol–gel method [6,7] and the hydrothermal [8,9] or solvothermal methods [10].

TiO_2 has the advantage of good chemical stability, absence of toxicity and relative low price, but a serious disadvantage is its large band-gap ($E_g = 3.2$ eV) that requires that near-UV light is used to photoactivate this very attractive photocatalyst. Many techniques have been examined to extend the spectral response of TiO_2 into the visible region and enhance its photocatalytic activity. Recently, improved TiO_2 photocatalysts have been obtained by doping with non-metal atoms such as carbon [11–14], nitrogen [14,15], sulfur [14,16] or using codoped materials [14,17–19]. Several attempts have been also made to narrow the band gap energy by doping with various transition metals ions [20–23] and lanthanides [24,25]. At this regard, great attention has been dedicated to vanadium (V)-doped titania, for which the preparation procedure has dramatic effects on the reactivity. As a matter of fact, while several works show that V-doped TiO_2 has an increased photoactivity with respect to the undoped sample [26–28], there are same evidences that V-doped TiO_2 produced by a co-precipitation method yields to opposite performances [29]. More recently, promising bulk boron (B)-doped TiO_2 has been investigated [30,31]. Here we present results relative to the design of improved TiO_2 photocatalysts doped with

* Corresponding author. Fax: +39 045 802 7929.
** Corresponding author. Fax: +39 040 558 3903.
*** Corresponding author. Fax: +39 045 802 7929.
E-mail addresses: marco.bettinelli@univr.it (M. Bettinelli), valerio.dallacasa@univr.it (V. Dallacasa), pfornasiero@units.it (P. Fornasiero).

0304-3894/$ – see front matter © 2007 Elsevier B.V. All rights reserved.
doi:10.1016/j.jhazmat.2007.04.053

V or B and we test their activity on the basis of the degradation of methylene blue (MB).

2. Experimental/material and methods

2.1. Reagents

Titanium(IV) butoxide ($Ti(OBu)_4$, 97%) and V oxytripropoxide ($VO(OPr)_3$, 98%) were from Aldrich, chloridric acid (HCl, 37%) and ethanol (EtOH, ≥ 99.9%) were from J.T. Baker, nitric acid (HNO_3, ≥ 65%) was from Fluka and boric acid (H_3BO_3, 99.8%) was from CarloErba. The water was distilled twice before use. All chemicals were used as received.

2.2. Catalyst preparation

2.2.1. V-doped samples

V-doped TiO_2 samples were prepared by a sol–gel method as follows. 30.0 mL of ethanol, 0.8 mL of HCl, 6.0 mL of $Ti(OBu)_4$ were mixed under stirring. The vanadium alkoxide was added at different times: after 1 min, 5 min, 30 min, 1 h and the samples will be denoted hereafter as TV1m, TV5m, TV30m, TV1h, respectively. The solvent was evaporated at 60 °C until the xerogels were formed. The xerogels were annealed in air at a temperature of 500 °C for 5 h and yellow–brown powders were obtained. In all cases the nominal molar ratio between titanium and vanadium was 99:1. For the sake of comparison, an undoped titania sample, labeled as TiO_2(I), was also prepared using the same procedure.

2.2.2. B-doped samples

B-doped TiO_2 samples were prepared by a sol–gel method as follows. Typically, 17.0 g of $Ti(OBu)_4$ were dissolved at 25 °C in 40.0 mL of anhydrous ethanol under argon atmosphere to form the solution 1. Meanwhile, 3.0 mL of concentrated HNO_3 were mixed with 35.0 mL of anhydrous ethanol and 15.0 mL of water to prepare the solution 2. Then the solution 1 was added drop-wise into the solution 2, under argon atmosphere, within 20 min under vigorous stirring. Appropriate amounts of H_3BO_3 were dissolved in 10.0 mL of bi-distilled water, and rapidly added drop-wise to the resulting solution. The solution was continuously stirred for 30–60 min until the formation of TiO_2 gel. After aging for at least 24 h at room temperature, the as-prepared TiO_2 gel was dried at 120 °C for 12 h. The obtained solid was ground and annealed at 450 °C for 6 h with a heating rate of 3 °C/min. For the sake of comparison, an undoped titania sample, labelled as TiO_2(II), was also prepared using the same procedure. The B-doped samples are denoted as TiO_2-X, where "X" represents the doping element B and the molar% nominal dopant loading.

2.3. Catalyst characterization

The specific surface areas of the samples (BET method) were obtained by N_2 physisorption at liquid nitrogen temperature using a Micromeritics ASAP2020C apparatus. All the samples were previously degassed at 350 °C for 12 h. Powder X-ray diffraction (XRD) patterns of the samples after annealing were recorded with a computer controlled Philips X'Pert diffractometer using Cu Kα radiation. Room temperature FT-Raman spectra were obtained using a Perkin-Elmer 2000 FT-Raman spectrometer equipped with an InGaAs detector. A diode pumped Nd:YAG laser (at 1064 nm), with a laser power of 300 mW, was used as the excitation source.

2.4. Photocatalysis experiments

The photocatalytic activity of the materials was tested with the degradation of MB. Experiments were carried out in a 450 mL Pyrex photochemical reactor with a 450 W medium pressure mercury lamp (model 7825–34, ACE GLASS Inc., USA). The initial concentration of the dye was 19 mg/L and the concentration of the photocatalyst was 2.8 g/L. The concentration of the TiO_2 photocatalyst was chosen as the minimum concentration to obtain full absorption of the incident photon flux. The degradation was carried out at 25 °C. The addition of the TiO_2 based catalysts induced a pH decrease to 5.5 in all cases. No significant modification of the pH was observed during the experiments. Cold aqueous potassium dichromate solution (3% w/w) was circulated through a cylindrical jacket, made of Pyrex and located around the lamp to filter the radiation with $\lambda < 420$ nm and to avoid the heating of solution. In this condition, the lamp yielded a photon flux of $\phi_i = 0.5\ mW\ cm^{-2}$, at $\lambda = 360$ nm and of $\phi_i = 108.0\ mW\ cm^{-2}$ in the spectral range between 400 and 1050 nm determined by using a DeltaOHM radiometer HD2302.0 leaned against the external wall of the photoreactor containing only pure water, whereas $\phi_i = 0.1\ mW\ cm^{-2}$ at $\lambda = 360$ nm and $\phi_i = 5\ mW\ cm^{-2}$ in the visible region was measured in the presence of the catalyst suspension. Before irradiation the suspension was stirred in the dark for 1 h to reach adsorption equilibrium [32]. In the case of B-doped TiO_2, The maximum decrease of the dye concentration due to this phenomenon was about 2–3%, while in the case of V-doped TiO_2 a significantly higher adsorption of MB on the TiO_2 surface was observed (15–30%). At each time step, an aliquot of 3.0 mL of the aqueous suspension was taken and filtered through a 0.45 μm millipore disc to remove the catalyst powder. A Perkin Elmer Lambda 2 UV–vis. spectrometer was used for the determination of dye concentration. Since the degradation pathway for the selected dye is known with high reliability [33,34], we have monitored only the decoloration process. The normalized intensity of the absorption band at 660 nm is therefore plotted as a function of time of irradiation.

3. Results and discussion

3.1. Characterization

It is widely accepted that the efficiency of TiO_2 as a photocatalyst is strongly related to its crystal structure. Titanium dioxide has three polymorphs: rutile (tetragonal, space group $P4_2/mnm$), anatase (tetragonal, space group $I4_1/amd$) and brookite (orthorhombic, space group $Pbca$) [35]. Under ambient conditions bulk rutile is thermodynamically more stable than anatase or brookite. However, the phase stability depends upon

Table 1
Texture and structural properties of TiO_2 and V and B-doped TiO_2

Sample	BET surface area (m^2/g)	Cumulative pore volume (mL/g)	Pore diameter (nm)	Crystallite size[a] (nm)	Anatase (%)	Rutile (%)
TiO_2 (II)	83	0.16	5.7	13	100	–
TiO_2–B2	86	0.13	4.1	A 8 R 22	97	3
TiO_2–B9	127	0.26	3.1	A 6 R 6	94	6
TiO_2–B18	139	0.26	5.2	A 5.9 R 10.5	79	21
TiO_2 (I)	58	0.12	5.4	12	100	–
T1V1m	58	0.14	7.3	12	100	–
T1V30m	85	0.18	6.0	12	100	–
T1V1h	107	0.22	6.2	12	100	–

[a] Obtained by Scherrer equation and the labels A and R refer to anatase and rutile respectively.

surface energy differences between the three phases and anatase with particle size below ca. 14 nm is more stable than rutile [36]. Also, anatase phase is more stable than brookite in nanocrystals with size smaller than 11 nm [37]. It is well documented that the anatase polymorph has a higher photoactivity compared to rutile or brookite polymorphs [1,4,38].

The sol–gel synthesis is an easy and rapid method to obtain single phase anatase TiO_2 [39–41], which may be also successfully doped with metal or non-metal ions [25,26,30,42]. By applying the sol–gel method we have obtained nanocrystalline TiO_2 powders doped with either B or V.

In the case of V, the vanadium precursor was added at different times during the sol–gel hydrolysis reaction. This procedure should produce TiO_2 samples with different distribution of the vanadium ions in the nanoparticle. In particular, the V ions should be more concentrated on the surface of the nanoparticles for samples in which the addition of the V precursor has been made at longer times. Table 1 summarize the XRD data and the texture characteristics (BET surface area and porosity). The phase contents of the samples were calculated from the integrated intensities of anatase and rutile diffraction peaks according to the following formula [37]:

$$W_R = \frac{A_R}{0.884A_A + A_R}$$

where W_R represents the weight fraction of rutile, A_A the integrated intensity of the anatase (1 0 1) peak and A_R the integrated intensity of the rutile (1 1 0) peak. The X-ray diffraction patterns indicate that the present V-doped samples consist of anatase single phase, with no contamination of other titania phases. This is also confirmed by Raman spectroscopy (see Fig. 1), a technique that can indicate the presence of additional phases (rutile or brookite) even at very low levels. In fact the Raman spectrum of anatase single crystal shows six Raman bands at 144 (E_g), 197 (E_g), 399 (B_{1g}), 513 (A_{1g}), 519 (B_{1g}) and 639 cm^{-1} (E_g) [38]. On the other hand, the rutile phase has four Raman active modes at 143 (B_{1g}), 447 (E_g), 612 (A_{1g}), and 826 cm^{-1}(B_{2g}) [39]. The brookite phase has three Raman bands at 366, 326 and 247 cm^{-1} [43,44]. The Raman spectra of the B-doped samples show the typical bands of the anatase phase (see Fig. 1). In addition, some bands at 447 and 612 cm^{-1}, due to the rutile phase, appear in the Raman spectra, giving rise to a broadening of the Raman bands. This evidence is more appreciable in the case of TiO_2–B18 sample, which contains the highest percentage of the rutile phase (21%, as indicated by the X-ray data, see Table 1). As already discussed in the literature [43,45], the Raman bands of rutile are broader in a mixed phase spectrum in which rutile is present as a minor component. Both the XRD and Raman data show that the presence of boron promotes the formation of the rutile phase.

The adopted preparation methods lead to the formation of mesoporous materials, all characterized by high surface area (Table 1). The addition of V after the hydrolysis of the titanium alkoxides enhances the surface area and porosity of the doped titania. The effect is more pronounced when the V addition is performed at higher hydrolysis degree, corresponding to higher

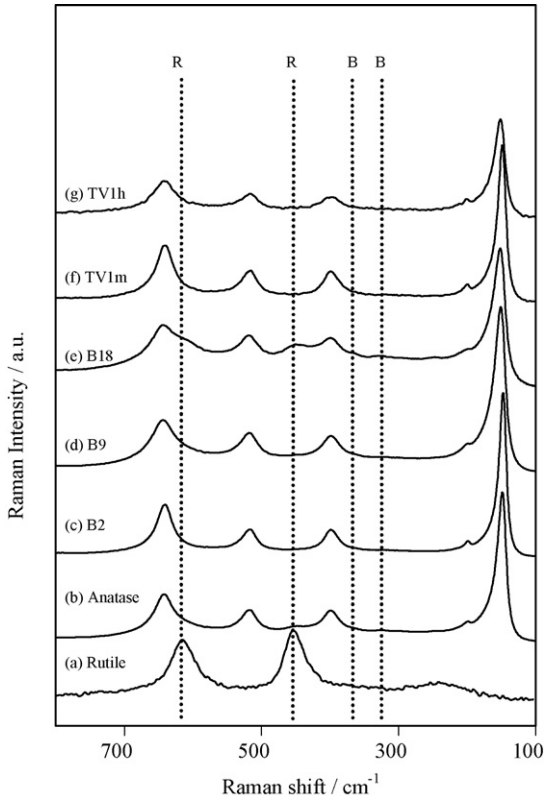

Fig. 1. Selected Raman spectra of TiO_2 samples: (a) TiO_2 (rutile), (b) TiO_2 (anatase), (c) TiO_2–B2, (d) TiO_2–B9, (e) TiO_2–B18, (f) TV1m and (g) TV1h. Dashed vertical lines indicate the position of rutile (R) and brookite (B) Raman peaks.

surface V concentration. The addition of growing quantities of B increases the surface area of the final materials. (Table 1)

3.2. MB photodegradation

The photocatalytic activity of the various TiO_2 systems was tested with the degradation of MB. Under the adopted experimental conditions, the degradation of the selected dye is significant only when TiO_2 and irradiation are simultaneously present.

Fig. 2 reports the MB degradation activity of TiO_2 and V-doped TiO_2 after 240 min of irradiation as a function of the preparation procedure. It must be noted that the MB adsorption on the catalyst surface is significant and depends on the preparation method. In fact adsorption of 27, 45, 38, 13 and 10% was observed respectively for TiO_2(I), TV1m, TV5m, TV30m and TV1h. Mutual interaction between Ti^{4+}/Ti^{3+} and V^{5+}/V^{4+} was deeply investigated by Trifirò et al. [46]. It has been indicated that complex redox process involving these species can modify the nature of the TiO_2 surface [47] and therefore the adsorption capacity. The MB photodegradation, after correction for the dye adsorption, indicates that the addition of 1 mol% vanadium during the sol–gel process (mainly in the bulk) does not influence the reactivity significantly, while the presence of V on the surface and the consequent increasing of sample surface area improve the photoreactivity. It is worth noting that when V is mainly present on the surface (TV1h sample) deactivation start to occur even thought the sample surface area is the highest of all the V-doped samples, suggesting the presence of some poisoning effects.

In agreement with previous observations [30], addition of bulk B enhances the photodegradation activity of the TiO_2 (Fig. 3). While the incorporation of 2 mol% of B has a minor effect, significant improvements are observed after doping TiO_2 with 9 and 18 mol% of B.

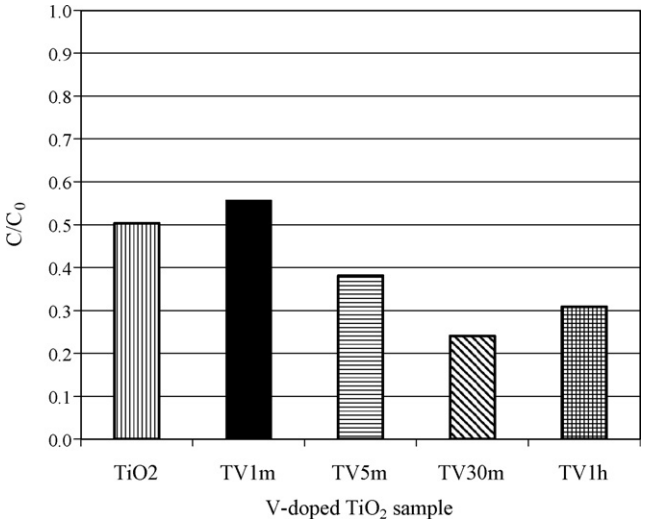

Fig. 2. Photocatalytic degradation of MB over V-doped TiO_2 after 240 min of irradiation. (a) TiO_2(I), (b) TV1m, (c) TV5m, (d) TV30m and (e) TV1h. Conditions: $C_0 = 19$ mg/L, m (TiO_2) = 1000 mg, $V = 350$ mL, $T = 25\,^{\circ}C$, natural pH.

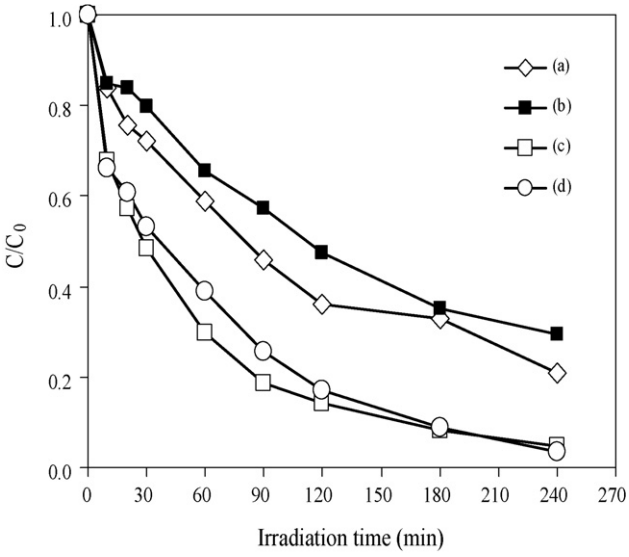

Fig. 3. Photocatalytic degradation of MB over B-doped TiO_2. (a) = TiO_2(II), (b) TiO_2–B2, (c) TiO_2–B9 and (d) TiO_2–B18. Conditions: $C_0 = 19$ mg/L, m(TiO_2) = 1000 mg, $V = 350$ mL, $T = 25\,^{\circ}C$, natural pH.

The improved photocatalytic activity of the B-doped TiO_2 is consistent with recent reports [11,12]. Our recent DFT calculations on 4 mol% B-doped TiO_2, predict an increased band gap for interstitial B-doped TiO_2 [48]. The calculated DOS indicates the presence of three partially reduced Ti sites for each introduced B as an interstitial dopant. A reduced Ti center on the TiO_2 surface was recently demonstrated to be the site for activation of highly reactive super-oxide species [14].

4. Conclusions

We have presented in this paper photocatalysis results for doping processes of TiO_2 based materials. The addition of 1 mol% of V can enhance the photodegradation of MB. More specifically, the data indicate that the activity can be tuned by dosing the amount of surface V. Above a certain concentration, deactivation was observed. More effective is bulk TiO_2 B-doping, leading to a significant enhancement of MB conversion. 9 mol% B was identified as the optimal composition for best photodegradation performances.

Acknowledgements

We are indebted to Prof. M. Graziani for numerous fruitful discussions and we are grateful to Prof. S. Enzo for the XRD measurements.

Universities of Trieste and Verona, Fondazione Cariverona, CENMAT, INSTM and FISR2002 “Nanosistemi inorganici ed ibridi per lo sviluppo e l’innovazione di celle a combustibile” are acknowledged for financial support.

References

[1] O. Carp, C.L. Huisman, A. Reller, Photoinduced reactivity of titanium dioxide, Prog. Solid State Chem. 32 (2004) 33–177.

[2] M.R. Hoffmann, S.T. Martin, W.Y. Choi, D.W. Bahnemann, Environmental applications of semiconductor photocatalysis, Chem. Rev. 95 (1995) 69–96.
[3] A. Fujishima, K. Honda, Electrochemical photolysis of water at a semiconductor electrode, Nature 238 (1972) 37–38.
[4] J. Augustynski, The role of the surface intermediates in the photoelectrochemical behavior of anatase and rutile TiO_2, Electrochim. Acta 38 (1993) 43–46.
[5] K.K. Akurati, S.S. Bhattacharya, M. Winterer, H. Hahn, Synthesis, characterization and sintering of nanocrystalline titania powders produced by chemical vapour synthesis, J. Phys. D: Appl. Phys. 39 (2006) 2248–2254.
[6] E. Pelizzetti, C. Minero, E. Borgarello, L. Tinucci, N. Serpone, Photocatalytic Activity, Selectivity of titania colloids and particles prepared by the sol–gel technique — photooxidation of phenol and atrazine, Langmuir 9 (1993) 2995–3001.
[7] R. Campostrini, G. Carturan, L. Palmisano, M. Schiavello, A. Sclafani, sol–gel derived anatase TiO_2 — morphology and photoactivity, Mater. Chem. Phys. 38 (1994) 277–283.
[8] M. Inagaki, Y. Nakazawa, M. Hirano, Y. Kobayashi, M. Toyoda, Preparation of stable anatase-type TiO_2 and its photocatalytic performance, Int. J. Inorg. Mater. 3 (2001) 809–811.
[9] J. Ovenstone, Preparation of novel titania photocatalysts with high activity, J. Mater. Sci. 36 (2001) 1325–1329.
[10] C.S. Kim, B.K. Moon, J.H. Park, S.T. Chung, S.M. Son, Synthesis of nanocrystalline TiO_2 in toluene by a solvothermal route, J. Cryst. Growth 254 (2003) 405–410.
[11] H. Irie, Y. Watanabe, K. Hashimoto, Carbon-doped anatase TiO_2 powders as a visible light-sensitive photocatalyst, Chem. Lett. 32 (2003) 772–773.
[12] M. Shen, Z.Y. Wu, H. Huang, Y.K. Du, Z.G. Zou, P. Yang, Carbon-doped anatase TiO_2 obtained from TiC for photocatalysis under visible light irradiation, Mater. Lett. 60 (2006) 693–697.
[13] C. Di Valentin, G. Pacchioni, A. Selloni, Theory of carbon doping of titanium dioxide, Chem. Mater. 17 (2005) 6656–6665.
[14] K.M. Reddy, B. Baruwati, M. Jayalakshmi, M.M. Rao, S.V. Manorama, S-, N- and C-doped titanium dioxide nanoparticles: synthesis, characterization and redox charge transfer study, J. Solid State Chem. 178 (2005) 3352–3358.
[15] S. Sakthivel, H. Kisch, Photocatalytic and photoelectrochemical properties of nitrogen-doped titanium dioxide, Chem. Phys. Chem. 4 (2003) 487–490.
[16] T. Ohno, M. Akiyoshi, T. Umebayashi, K. Asai, T. Mitsui, M. Matsumura, Preparation of s-doped TiO_2 photocatalysts and their photocatalytic activities under visible light, Appl. Catal., A 265 (2004) 115–121.
[17] Y. Cong, F. Chen, J.L. Zhang, M. Anpo, Carbon and nitrogen-codoped TiO_2 with high visible light photocatalytic activity, Chem. Lett. 35 (2006) 800–801.
[18] H.Q. Sun, Y. Bai, Y.P. Cheng, W.Q. Jin, N.P. Xu, Preparation and characterization of visible light-driven carbon–sulfur codoped TiO_2 photocatalysts, Ind. Eng. Chem. Res. 45 (2006) 4971–4976.
[19] D. Noguchi, Y. Kawamata, T. Nagatomo, The response of TiO_2 photocatalysts codoped with nitrogen and carbon to visible light, J. Electrochem. Soc. 152 (2005) D124–D129.
[20] M.I. Litter, J.A. Navio, Comparison of the photocatalytic efficiency of TiO_2 iron-oxides and mixed Ti(IV) Fe(III) oxides - photodegradation of oligocarboxylic acids, J. Photochem. Photobiol. A: Chem. 84 (1994) 183–193.
[21] K. Wilke, H.D. Breuer, Transition metal doped titania: physical properties and photocatalytic behaviour, Z. Phys. Chem.– Int. J. Res. Phys. Chem. Chem. Phys. 213 (1999) 135–140.
[22] A. Sclafani, L. Palmisano, E. Davi, Photocatalytic degradation of phenol in aqueous polycrystalline TiO_2 dispersions — the influence of Fe^{3+}, Fe^{2+} and Ag^+ on the reaction rate, J. Photochem. Photobiol. A: Chem. 56 (1991) 113–123.
[23] Y.A. Cao, W.S. Yang, W.F. Zhang, G.Z. Liu, P.L. Yue, Improved photocatalytic activity of Sn^{4+} doped TiO_2 nanoparticulate films prepared by plasma-enhanced chemical vapor deposition, New J. Chem. 28 (2004) 218–222.
[24] M. Bettinelli, A. Speghini, D. Falcomer, M. Daldosso, V. Dallacasa, L. Romanò, Photocatalytic, spectroscopic and transport properties of lanthanide-doped TiO_2 nanocrystals, J. Phys.: Condens. Matter 18 (2006) S2149–S2160.
[25] A.W. Xu, Y. Gao, H.Q. Liu, The preparation, characterization, and their photocatalytic activities of rare earth-doped TiO_2 nanoparticles, J. Catal. 207 (2002) 151–157.
[26] S.M. Karvinen, The effects of trace element doping on the optical properties and photocatalytic activity of nanostructured titanium dioxide, Ind. Eng. Chem. Res. 42 (2003) 1035–1043.
[27] J.J. Shyue, M.R. De Guire, Single-step preparation of mesoporous, anatase-based titanium–vanadium oxide and its application, J. Am. Chem. Soc. 127 (2005) 12736–12742.
[28] M. Anpo, Y. Ichihashi, M. Takeuchi, H. Yamashita, Design of unique titanium oxide photocatalysts by an advanced metal ion-implantation method and photocatalytic reactions under visible light irradiation, Res. Chem. Intermed. 24 (1998) 143–149.
[29] S.T. Martin, C.L. Morrison, M.R. Hoffmann, Photochemical mechanism of size-quantized vanadium-doped TiO_2 particles, J. Phys. Chem. 98 (1994) 13695–13704.
[30] D. Chen, D. Yang, Q. Wang, Z.Y. Jiang, Effects of boron doping on photocatalytic activity and microstructure of titanium dioxide nanoparticles, Ind. Eng. Chem. Res. 45 (2006) 4110–4116.
[31] W. Zhao, W.H. Ma, C.C. Chen, J.C. Zhao, Z.G. Shuai, Efficient degradation of toxic organic pollutants with $Ni_2O_3/TiO_{2-x}B_x$ under visible irradiation, J. Am. Chem. Soc. 126 (2004) 4782–4783.
[32] H. Lachheb, E. Puzenat, A. Houas, M. Ksibi, E. Elaloui, C. Guillard, J.M. Herrmann, Photocatalytic degradation of various types of dyes (alizarin S, crocein orange G, methyl red, congo red, methylene blue) in water by UV-irradiated titania, Appl. Catal., B 39 (2002) 75–90.
[33] C. Baiocchi, M.C. Brussino, E. Pramauro, A.B. Prevot, L. Palmisano, G. Marci, Characterization of methyl orange and its photocatalytic degradation products by HPLC/UV–vis diode array and atmospheric pressure ionization quadrupole ion trap mass spectrometry, Int. J. Mass Spectrom. 214 (2002) 247–256.
[34] A. Houas, H. Lachheb, M. Ksibi, E. Elaloui, C. Guillard, J.M. Herrmann, Photocatalytic degradation pathway of methylene blue in water, Appl. Catal., B 31 (2001) 145–157.
[35] J. Ovenstone, K. Yanagisawa, Effect of hydrothermal treatment of amorphous titania on the phase change from anatase to rutile during calcination, Chem. Mater. 11 (1999) 2770–2774.
[36] H.Z. Zhang, J.F. Banfield, Thermodynamic analysis of phase stability of nanocrystalline titania, J. Mater. Chem. 8 (1998) 2073–2076.
[37] H.Z. Zhang, J.F. Banfield, Understanding polymorphic phase transformation behavior during growth of nanocrystalline aggregates: insights from TiO_2, J. Phys. Chem. B 104 (2000) 3481–3487.
[38] K. Yanagisawa, J. Ovenstone, Crystallization of anatase from amorphous titania using the hydrothermal technique: effects of starting material and temperature, J. Phys. Chem. B 103 (1999) 7781–7787.
[39] K.L. Frindell, M.H. Bartl, A. Popitsch, G.D. Stucky, Sensitized luminescence of trivalent europium by three-dimensionally arranged anatase nanocrystals in mesostructured titania thin films, Angew. Chem. Int. Ed. 41 (2002) 959-962.
[40] K. Wilke, H.D. Breuer, The influence of transition metal doping on the physical and photocatalytic properties of titania, J. Photochem. Photobiol. A: Chem. 121 (1999) 49–53.
[41] M.S.P. Francisco, V.R. Mastelaro, Inhibition of the anatase–rutile phase transformation with addition of CeO_2 to $CuO–TiO_2$ system: Raman spectroscopy, X-ray diffraction, and textural studies, Chem. Mater. 14 (2002) 2514–2518.
[42] H. Wang, J.P. Lewis, Second-generation photocatalytic materials: anion-doped TiO_2, J. Phys.: Condens. Matter 18 (2006) 421–434.
[43] M.P. Moret, R. Zallen, D.P. Vijay, S.B. Desu, Brookite-rich titania films made by pulsed laser deposition, Thin Solid Films 366 (2000) 8–10.

[44] G.A. Tompsett, G.A. Bowmaker, R.P. Cooney, J.B. Metson, K.A. Rodgers, J.M. Seakins, The Raman-Spectrum of brookite, TiO_2 (Pbca, $Z = 8$), J. Raman Spectrosc. 26 (1995) 57–62.
[45] R.J. Betsch, H.L. Park, W.B. White, Raman-Spectra of stoichiometric and defect rutile, Mater. Res. Bull. 26 (1991) 613–622.
[46] F. Trifirò, The chemistry of oxidation catalysts based on mixed oxides, Catal. Today 41 (1998) 21–35.
[47] J.M. Herrmann, J. Disdier, G. Deo, I.E. Wachs, Semi-conductive and redox properties of V_2O_5/TiO_2 catalysts, J Chem. Soc. 93 (1997) 1655–1660.
[48] G. Vicario, PhD Thesis, University of Trieste, (2007).